Simulating Injectate/Rock Chemical Interaction In Fractured Desert Peak Quartz Monzonite

B.E. Viani, J.J. Roberts, R.L. Detwiler, S.K. Roberts, S.R. Carlson

June 2, 2005

Disclaimer

Simulating Injectate/Rock Chemical Interaction In Fractured Desert Peak Quartz Monzonite

Brian E. Viani, Jeffery J. Roberts, Russell L. Detwiler, Sarah K. Roberts, and Steven R. Carlson

Lawrence Livermore National Laboratory
Livermore, CA 94551

Key words: fracture permeability, fluid-rock interaction, geochemical modeling, Desert Peak, enhanced geothermal systems, EGS

Abstract

Simulations of the interactions of injected fluids with minerals within an engineered fracture in a sample of Desert Peak quartz monzonite were compared with experimental observations of fluid chemistry and fracture permeability. The observed decrease in permeability and effective hydraulic aperture was much more rapid (~1.0 μm/day) for a core injected with a mixed salt solution containing dissolved silica (near-saturation injectate), compared to cores injected with NaCl (far-from-saturation injectate) (~0.1 μm/day). Simulations were in qualitative agreement with these observations. Near-saturation injectate is predicted to result in net *precipitation* of secondary phases in the fracture (~0.12 μm/day), compared to a net *dissolution* of the rock for the far-from-saturation injectate (~0.3 μm/day). Permeability loss for the near-saturation-injectate is ascribed to precipitation in the fracture as well as potential dissolution of primary mineral asperities. Permeability loss for the far-from-saturation fluid is ascribed to dissolution of asperities and smoothing of the fracture. Post-test analysis of the fracture surface will be necessary to verify the processes occurring. The simplified geochemical models used do not account for mineral heterogeneity or for distributions of fluid residence times which could be important controls on permeability evolution.   Further analysis is planned to explicitly account for these phenomena.

Introduction

Increasing the permeability and heat transfer of geothermal reservoirs by creating new fractures and maintaining the permeability of existing fractures during injection of produced or surface waters is a pre-requisite for maintaining and enhancing resource production. Because injected fluids are likely to be out of equilibrium with minerals exposed by fracturing, there is a potential to negatively impact the reservoir if injected fluids cause or increase the rate of fracture sealing due to either precipitation of minerals in the fractures, or dissolution of asperities that may be propping the fracture open. Geochemical modeling simulations provide a means for comparing and evaluating various hypotheses that have been put forward to explain the variation in permeability during the flow of fluids through fractures. With sufficient validation and verification, geochemical modeling could be used to chemically engineer benign (or even beneficial) reinjection fluids. In this study, geochemical modeling was used to help assess the impact of water-rock interaction on physical changes observed during isothermal fluid transport through a fractured monzonite core from the Desert Peak East enhanced geothermal system test site. We present results of simulating chemical reaction between injectate fluids and fracture-

wall phases at a temperature of 167 ºC and confining pressures of 3.4-3.8 MPa. We compare our results with experimental observations reported by Carlson et al. (2005}.

Flow experiments

Carlson et al. (2005) observed changes in resistivity and permeability accompanying fluid flow through fractures created in cylindrical cores (25.4 mm diameter x 43 mm long) maintained at 167-169 ºC for periods ranging from 37 to 111 days. Fluid was injected into the core samples under constant flux (between 0.005 and 0.2 mL min). The permeability of the cores was measured periodically during the experiment and an effective hydraulic aperture was calculated from this data. The effective hydraulic aperture is the aperture of a plane-parallel, smooth-walled fracture that is required to match the observed flux and pressure head. All flux is assumed to flow through a single fracture under steady state laminar flow conditions. The range of effective apertures measured for the 4 cores studied varied from a 36 to 5 μm (Table 1). In 3 of the 4 samples studied, the effective hydraulic aperture of the fracture decreased during the period of time fluid was injected into the core. (In the fourth sample, the starting aperture was not measured, and therefore the change in aperture could not be determined).

<INSERT TABLE 1 HERE>

Two types of fluids were used as injectates: a NaCl solution (far-from-equilibrium with the phases in the core ('far-from-saturation injectate')), and a mixed salt solution that also contained dissolved silica. The latter solution ('near-saturation injectate') is intended to simulate a silica-bearing fluid that might be re-injected into a geothermal reservoir. This fluid would be expected to be closer to equilibrium with the phases in the core. However, because the fluid reservoir in our experiments is not heated, the silica concentration in the fluid had to be maintained below the saturation of amorphous silica at ambient temperature. Hence, the silica concentration is lower than would be encountered in most re-injectates.

Experimental constraints and boundary conditions – As noted in Carlson et al. (2005), the bead-blasting method used to create one of the fracture surfaces produces a relatively reproducible surface topography. Some of this topography may be controlled by mineralogy (e.g., the observation that a healed fracture was more deeply eroded than surrounding minerals). The superposition of the rough surface with the smooth surface results in a fracture that creates a flow field that is not random (Carlson et al., 2005) (Figure 1). Based on this analysis, one would expect the flux field to display a distribution of fluid velocities and residence times.

<INSERT FIGURE 1 HERE>

Figure 1.   (a) Perspective view of fracture aperture calculated from high-resolution surface profilometry (30x vertical exaggeration). (b) Gray-scale image of fracture apertures (scale 0.0 mm (black); 0.25 mm (white)). (c) Simulations of fluid flow through the fracture yield estimates of local fluxes where the gray-scale (black through white) represents increasing fluxes. Flow direction is from top to bottom.

Experimental observations: comparison between far-from-saturation injectate (NaCl; DP3972.3) and near-saturation injectate (mixed salt plus silica; DP3972.4) flow tests -- Over a

period of 65 days a NaCl solution was passed through core DP3972.3. During this period, two observations may at least partly be attributable to fluid-rock reactions. (1) Based on resistivity and differential pressure measurements, permeability (k) decreased continuously during flow. Hydraulic aperture decreased about 20%. (2) During periods (several days) of no-flow (shut-in), the resistivity of the core decreased approximately exponentially with a half-life on the order of 15 to 20 hours. Permeability and hydraulic aperture also decreased for sample DP3972.4 (near-saturation-injectate). However, the rate of aperture reduction was about an order of magnitude faster (Table 1). Details of these experiments are described in Carlson et al. (2005).

Fracture apertures and fluid residence times – For the core geometry used, and a flow rate of 0.02 mL/min (the predominant flow rate used during the experiments), the <u>average</u> residence time of the fluid in the fracture would be 0.215 and 2.15 min for 4 and 40-μm effective apertures, respectively. At the lowest flow rate used (0.005 mL/min), the residence time could be as long as 8.6 min for a 40 μm aperture; at the highest flow rate (0.2 mL/min) the residence time could be as short as 0.022 min for a 4 μm aperture.

Injectate and effluent fluid analyses – Chemical analysis of the injectate and effluent was made only for the DP3972.4 core that was subjected to the near-saturation injectate (Table 2). No samples were collected for previous runs (provision for sampling the effluent under pressure was not available). Standard instrumental methods of analysis (inductively coupled plasma spectroscopy, ion chromatography) were used for analyzing the fluids. For most samples, analysis of unfiltered and filtered samples was made to assess whether colloidal precipitates were present. There did not appear to be any significant differences in filtered and unfiltered samples. Hence, the data presented in Table 2 represents averages of analyses for filtered and unfiltered aliquots. Effluent samples were collected at pore pressure using a stainless-steel syringe pump.

With the exception of dissolved inorganic carbon (HCO_3) there does not appear to be a clear trend with time for the effluents analyzed. We note that the influent HCO_3 concentration also decreased with time (not shown). Hence, there appears to have been some degassing of CO_2 from the reservoir during the run. Effluent concentrations are similar to influent concentrations. Although the effluent pH measured at ambient temperature is about 1 pH unit higher than the effluent pH calculated at 167 ºC (Table 2), simulations show that this difference is mainly due to the temperature difference between measurement and calculation, and not due to compositional differences between simulated and actual effluents.

<INSERT TABLE 2 HERE>

Conceptual models of permeability changes during fracture flow

We assume that the major geochemical processes that could impact the evolution of fracture permeability in our core flow tests are dissolution of fracture wall minerals or precipitation of minerals within the fracture. Other potential geochemical processes, such as clay swelling, colloid entrainment and entrapment are not expected to play an important role under the temperature-time-pressure, regime imposed, and fluid and rock compositions used in the experiment. Chemically enhanced subcritical crack growth could impact the rate at which asperities are broken down under confining pressure. We do not explicitly address this process,

but note that fracture fluid chemistry could potentially impact the rate of subcritical fracture growth. Hence, understanding the chemistry of fluids in fractures might be necessary to assess the role of subcritical crack growth in asperity breakdown.

Injectate fluid far-from-saturation with respect to minerals in the fracture – For fluids that are undersaturated with respect to the solid phases in the rock, dissolution processes will dominate. However, the effect of dissolution on fracture permeability can differ, depending on the mineralogic heterogeneity of the rock in question.

For a fracture created in a monomineralic rock in which the fracture aperture is supported against closure (under a confining pressure) by topographic asperities, a fluid that is undersaturated with respect to the mineral constituent of the rock, would dissolve both asperities and non-asperity regions of the fracture wall, and result in a decrease in permeability as the fracture surface becomes smoother and the aperture closes under confining pressure. However, if the imposed heterogeneous flow lines govern the overall extent of dissolution (because of differences in residence times), then a few channels may dominate the flux, and hence the dissolution. If the main flow-bearing channels broaden, smoothing and permeability decreases could be expected. If the main flow-bearing channels become entrenched into the fracture wall, permeability may stabilize.

For a fracture developed in a polymineralic rock, a similar process could occur, but in addition, there is a potential for developing preferred flow paths via differential dissolution (i.e., the formation of channels) of more rapidly dissolving (or more soluble) phases. Under conditions where channel development exceeds asperity removal, undersaturated fluids could potentially increase permeability (similar to creating flow-path controlled entrenched flow channels in monomineralic rock). Hence, the evolution of permeability during flow of an 'aggressive' injectate will likely represent the net effect of smoothing and channeling.

Injectate fluid near, at, or above saturation with respect to minerals in the fracture – When a fluid that is slightly less than or at saturation with minerals lining the fracture, flows through the fracture, the rate at which smoothing or channeling occurs would be slower than for highly undersaturated fluids; hence the rate of change in permeability should be slower compared to an aggressive fluid. However, under conditions in which the fluid being put through the fracture is supersaturated with respect to minerals in the rock or other phases, there is a potential for precipitation in the fracture, and a consequent decrease in permeability as the fracture fills. A variant of this scenario is the case where the fluid becomes supersaturated with respect to a secondary mineral, even as it remains undersaturated with respect to the primary minerals in the rock. In this scenario, both dissolution of the primary rock minerals and precipitation of secondary phases could occur, and the net effect on permeability will depend on the relative masses and volumes of the minerals dissolved and precipitated, and their location in the fracture. This scenario is in fact, predicted by the geochemical modeling simulation for the near-saturation fluid. The loci of precipitation of phases will depend on the fluid velocity and residence time distribution. It could be hypothesized that precipitation from a supersaturated fluid injectate would be most likely in the smallest flow channels (longest residence times). However, for the case where dissolution of the primary minerals is driving the precipitation of secondary minerals, more precipitation could potentially occur in the higher flux flow paths.

Geochemical modeling simulations for the fractured monzonite core sample

The geochemical modeling program (REACT) (Bethke, 2004) was used to simulate fluid-rock interaction within the fracture. This program can calculate the equilibrium distribution of aqueous species and mineral phases based on thermodynamic data. With appropriate kinetic data, it can also calculate the rates of mineral dissolution and precipitation for systems that are not at equilibrium.

Kinetic constraints on injectate/rock interaction – In order to calculate the extent of mineral dissolution during the passage of fluid through a fractured rock, the rate of mineral dissolution as a function of temperature, fluid composition, and surface area must be known. Except for very simple systems, insufficient data is available to quantitatively predict the rates of mineral dissolution. However, existing data is sufficient to be used to qualitatively assess whether the fluid in a fractured system is likely to equilibrate with fracture wall minerals during fluid flow.

A simplified rate law was used to compute mineral dissolution under conditions where the pH of the fluid remains approximately constant:

$$r = k S \left[\frac{Q}{K} - 1 \right], \qquad \text{where} \qquad k = A \exp \left[\frac{-E_a}{RT} \right], \qquad [1]$$

and r is the dissolution rate (mol/s), k is the rate constant (mol/cm^2-s), S is the surface area (cm^2), Q is the dissolution reaction quotient, K is the equilibrium constant (Q/K is the saturation index of the fluid with respect to the mineral in question), A is the pre-exponential factor (mol/cm^2-s), E_a is the activation energy for the dissolution reaction (J/mol), R is the gas constant (J/mol K), and T is the Kelvin temperature (K). This equation is strictly valid for the near neutral region where rates of dissolution are independent of pH.

Preliminary simulations suggested pH would remain between 7-8 during passage through the rock. In this pH region, dissolution rates are nearly independent of pH. However, post-modeling experimental results (Table 2), indicated that although the measured effluent pH was approximately constant (~9), the pH increased by as much as 1.4 pH units during passage through the rock. The dissolution rates predicted by this model therefore, provide a lower boundary to the actual rates for those minerals (primarily aluminosilicates) whose rates increase with increasing pH

Surface area to fluid volume relationships – For a given mineral mass and fluid composition, the rate of dissolution will depend on the surface area of the mineral exposed to the fluid. Rates of mineral equilibration with the fluid will depend on the ratio of its surface area to the volume of fluid it is in contact with. For a perfectly smooth fracture, the ratio of the geometric surface area to fluid volume would be 5 x 10^5 cm^2/L for a 40 μm and 5 x 10^6 cm^2/L for a 4 μm aperture. We assumed that the surface area for each mineral exposed to the fluid in the fracture was proportional to its mass fraction in the rock. Because one of fracture surfaces is not smooth (e.g., Figure 1), the assumed surface area to volume ratio is a lower bound. The degree of underestimation of surface area is not known, but will depend on the roughness of the fracture. The large surface area to volume ratios afforded by narrow apertures means that residence times

in fractures do not have to be very long for the fluid to approach equilibration with the fracture wall minerals.

We explicitly simulated the kinetics of dissolution and precipitation for the major minerals in monzonite: quartz, plagioclase (as a mixture of albite and anorthite) potassium feldspar, and biotite (Table 3). We also simulated dissolution and precipitation of calcite, which is found as a vein-filling phase in these rocks. The zeolite mesolite (a sodium calcium aluminosilicate) was also included in the simulation as a proxy for secondary zeolites that are reasonable phases to form at this temperature.

<INSERT TABLE 3 HERE>

Assumptions and methodology

The geochemical modeling program (REACT) (Bethke, 2004) was used to assess the degree to which injectate fluids approached equilibrium with the rock for various fluid residence periods. Mineral surface areas and dissolution rates were used as tabulated above. The calculations were made assuming a batch system; i.e., that the fluid and minerals were in contact with each other for a time period greater or equal to the calculated residence times based on the effective hydraulic aperture.

Modeling focused on two fluids (Table 2); the fluid used in initial experiments (far-from-saturation injectate, DP3972.3) and an injectate fluid that is more similar to proposed geothermal re-injection fluids, and that is much closer to equilibrium with respect to the major monzonite phases (near-saturation injectate, DP3972.4). The simulation temperature was 167 ºC, identical to the initial and current experiments. Simulations were performed in duplicate for each fluid/fracture aperture modeled; one simulation was made allowing the kinetically controlled precipitation of selected secondary phases; a duplicate simulation was made suppressing the precipitation of secondary phases (results not shown).

Simulation Results

Simulation outputs include predicted effluent compositions (Table 2), masses of minerals dissolved and precipitated vs. time, the net mass of material removed or added to the fracture (Figure 2), speciation of the aqueous phase, and saturation indices for all minerals in the composition space. In this report, only the masses of minerals precipitated or dissolved and net mass of material will be presented, as these are the critical parameters needed for predicting the average behavior of the system.

Far-from-saturation injectate – The far-from-saturation fluid is predicted to always dissolve the rock for residence times up to 5 minutes (Figures 2a,c). Although the mass of rock predicted to be removed in one residence time interval is small, over a 65-day period, approximately 28 g of material per square meter of fracture surface is predicted to be removed from a 40-μm fracture with a flux of 0.02 mL/min. This is equivalent to ~61 mg of material removed from the core sample (or ~10 μm of material removed from each face of the fracture, assuming an average density of 2.7 g/cm^3).

Based on the kinetic data in Table 1 (k_{167}), it is predicted that feldspar phases will dissolve more rapidly than quartz (Figure 2a). However, because quartz is a relatively minor component (7%) of this rock, its role in controlling fracture aperture may be less significant for this sample than for more quartz rich rocks such as granite. Note that channeling is not predicted for this system because the major phases (feldspars) have similar dissolution kinetics (Table 3). A significant fraction of the mass of rock removed by the dissolution is due to rapid dissolution of calcite very early in the reaction sequence. However, calcite is predicted to rapidly (within the first minute of fluid-rock contact) reach equilibrium with the fluid. Because calcite is not uniformly distributed in the core, one cannot necessarily conclude that dissolution of calcite is greatest at the front end of the core. The observed decrease in permeability for DP3972.1 and DP3972.3 is consistent with a generalized dissolution regime that results in the reduction of asperities and the creation of a smoother surface. The maintenance of a constant confining pressure presumably results in the closure of the aperture as asperities are dissolved. Apparently, channeling or differential dissolution, if it occurred was not sufficient to maintain or increase permeability,

<INSERT FIGURE 2 HERE)

Figure 2.   Comparison of mineral and rock mass changes per square meter of fracture surface vs. fluid residence time (40-mm aperture) due to mineral dissolution and precipitation in a fracture for far-from-saturation (a) and near-saturation (b) fluid injectates. Net mass of rock precipitated or removed is shown in (c). Negative values indicate dissolution; positive values indicate precipitation.

Near-saturation injectate – For the current experiment (DP3972.4), two outcomes are possible, depending on whether or not secondary mineral phases precipitate in the fracture. In the *absence of precipitation of secondary phases*, the mass of rock predicted to be removed (not shown) is much less than for the far-from-saturation injectate (by a factor of ~10 for a flow rate of 0.02 mL/min). Hence, permeability decline due to fracture surface smoothing should occur at a significantly slower rate than previously observed. If on the other hand, secondary minerals that are predicted to reach saturation, do precipitate in the fracture, permeability should decline much more rapidly than previously observed for the far-from-saturation injectate. This in fact, has been observed. The measured decrease in effective hydraulic aperture has been the most rapid and of the greatest magnitude of all the cores studied (Table 1). Simulations predict calcite rapidly precipitates as the fluid reacts with the core. Together with mesolite, approximately 0.4 mg/m^2 of precipitate is predicted per residence time interval (0.02 mL/min; Figure 2b). However, because significant quantities of feldspars are dissolved, the net amount of material added to the fracture is ~0.24 mg/m^2 per residence time period. Based on this simulation, the fracture aperture would be expected to be reduced by about 4.3 μm over 37 days the experiment has been run. This corresponds to about 0.06 μm/day of material *added* to each fracture surface, compared to 0.15 μm/day predicted to be *removed* from each surface for the far-from-saturation injectate. The rapid decrease in effective aperture (~1 μm/day) observed during the near-saturation injectate experiment (Table 1) is much greater than the decrease in aperture predicted due precipitation (0.12 μm/day). The extent of primary mineral dissolution (and hence of secondary mineral precipitation), as noted above, may be underestimated because of the underestimation of surface area, and because of the assumption of constant and near-neutral pH. However, aperture reduction could also occur via asperity destruction as primary minerals are dissolved. Clearly,

the location of dissolution and precipitation will control the net effect of chemical reaction. Post-test analysis will be necessary to assess the dominant processes occurring.

Simulating fluid compositional changes during shut-in – During several shut-in periods (no flow) for the far-from-saturation injectate, the resistivity was observed to decrease (Carlson et al., 2005). We hypothesized this decrease resulted from an increase in the concentration of electrolytes in the fluid as it equilibrated with the fracture minerals. A simulation of this process is qualitatively in line with this hypothesis, in that the fluid electrolyte concentration does increase (simulation not shown), and the rate of increase of this concentration occurs over a time scale similar to the observed decrease in resistivity. However, the predicted magnitude of the increase in the concentration of dissolved constituents appears to be too small to account for the observed resistivity decrease (TDS is predicted to increase by 150 to 350 mg/L after 80 hours of shut-in from an initial value ~8500 mg/L).

Conclusions

Geochemical modeling analysis of far-from-saturation and near-saturation injectate fluids showed:

1. Although residence times are short, reaction kinetics are predicted to be rapid enough to remove a significant mass of rock from the core for the far-from-saturation injection fluid (e.g., ~61 mg for 65 days @ 0.02 mL/min for a 40-mm aperture – equivalent to ~20 μm of rock or 0.3 μm/day). Near-saturation injectate is predicted to close the aperture by precipitating calcite and mesolite. This could decrease the aperture by about ~4.3 μm over a 37 day period (0.12 μm/day). The observed overall flow behavior of the cores for the two types of fluids is in general consistent with simulation results. However, until detailed post-test examination of the mineral surface is made, these results will not be able to be verified.

2. Simulated changes in fluid composition during shut-in show a similar rate to observed decreases in core resistivity, but the magnitude of the predicted increase in fluid electrolyte concentration does not seem large enough to account for the observed resistivity drop.

3. We recognize that, although this simplified batch model is adequate for predicting the average behavior of fluid-rock interaction in the fracture, it does not address the likely variation in residence times within the flow field that is suggested by an analysis of the surface topography (Figure 1). Nor does this approach address spatial heterogeneity in mineralogy, or the potential for spatial separation of dissolution regimes from precipitation regimes. However, this approach does provide a solid baseline for addressing these points in future studies.

Future work – Because flow simulation of fractured surfaces predict multiplicity of flow paths having a range of fluxes (i.e., residence times) (Figure 1), additional simulations will be undertaken that take account of the distribution of residence times. The kinetic model used to predict precipitation and dissolution will be improved by explicitly including pH dependence on rate constants and by using fracture characterization data to better constrain fracture surface area. We also plan to extend the modeling to include reactive transport along multiple 1-D flow paths having properties constrained by the flow simulation models derived from fracture topographic

analysis. This simulation will explicitly account for mineralogic heterogeneity along the flow path.

References

Bethke, C.M. 2004. The Geochemist's Workbench, Release 5.0, University of Illinois,.

Carlson, S.R., J.J. Roberts, R.L. Detwiler, B.E. Viani, and S.K. Roberts, 2005. Fracture Permeability in Desert Peak Quartz Monzonite, *Geothermal Resources Council Transactions*, V.29.

Sonnenthal, E., and N. Spycher. 2001. *Drift-Scale Coupled Processes (DST and THC Seepage) Models*. MDL-NBS-HS-000001 REV01 Bechtel, Las Vegas NV.

Table 1.   Calculated initial and final effective hydraulic apertures for Desert Peak fractured core samples.

Experiment	Duration	Initial Aperture	Final Aperture	Rate of Aperture Decrease	Fluid
	(day)	(μm)	(μm)	(μm/d)	
DP 3972.1	78	14.2	4.8	0.12	NaCl – *far-from-saturation injectate*
DP 3972.2	37	NA	18.6	-	NaCl – *far-from-saturation injectate*
DP 3972.3	65	32.9	26.1	0.1	NaCl – *far-from-saturation injectate*
DP 3972.4	In progress	36.1	8.3[1]	0.99	Mixed salts plus silica – *near-saturation injectate*

[1] This value was measured after 28 days of fluid injection.

Table 2.   Injectate and effluent fluid compositions from core samples DP3972.1-DP3972.4, and simulated effluent composition.

Constituent	Far-from-saturation injectate[1] mg/L	Near-saturation injectate (DP3972.4) Injectate[2] mg/L	Effluent day 21 mg/L	Effluent day 28 mg/L	Effluent day 35 mg/L	Predicted[3] effluent composition mg/L
Na	3344	3138 ± 25	2951	3035	2946	2987
K	0	386 ± 6	355	365	347	386
Ca	0	158 ± 1	143	161	149	152
SiO_2	0	81.6 ± 1.15	77.6	80.5	79.4	84.2
Cl	5156	5180 ± 117	4972	5070	4695	5180
HCO_3	NA	11.4 ± 5.7	46.5	30.8	14.3	5.08
TDS	8500	8955 ± 156	8545	8742	8231	8794
pH[4]	~6	8.06 ± 0.20	9.4	9.21	8.75	8.00

[1] This injectate used for experiments (DP 3972.1-3). No independent analyses of the injectate were made. The concentrations of Na and Cl are based on the measured mass of reagent; pH is assumed.

[2] This injectate is being used for experiment DP 3972.4 (concentrations are averages of analyses of influent solution at three different dates; day 21,28,35).

[3] The simulation was made according to the text. Starting fluid composition was set equal to the measured injectate composition for the near saturation injectate (column 3). The electrical balance for the solution was made by adjusting the Na concentration.

[4] All pH measurements were made at ambient temperature. The predicted pH of the effluent is the pH calculated for the effluent at the temperature of the experiment (167 ºC). The corresponding ambient-temperature pH is about 1 pH unit higher; i.e., ~9.

Table 3. Kinetic and surface area data used for simulating the interaction of monzonite with injected fluids[1].

Mineral	A (mol/cm^2-s)	E_a (J/mol)	k_{167}[2] (mol/cm^2-s)	Aperture = 40 μm	
				S (cm^2)	r (mol/s)
Quartz	2.69 x 10^{-3}	8.75 x 10^4	1.26 x 10^{-18}	4.54 x 10^4	5.04 x 10^{-9}
Anorthite	7.65 x 10^{-5}	6.78 x 10^4	1.0 x 10^{-16}	1.43 x 10^5	9.75 x 10^{-8}
Albite	7.65 x 10^{-5}	6.78 x 10^4	1.0 x 10^{-16}	1.43 x 10^5	9.75 x 10^{-8}
K-feldspar	1.33 x 10^{-6}	5.78 x 10^4	1.0 x 10^{-16}	1.49 x 10^5	2.76 x 10^{-8}
Biotite	1.13 x 10^{-4}	3.55 x 10^4	5.0 x 10^{-17}	1.95 x 10^4	9.41 x 10^{-9}
Calcite	3.46 x 10^{-3}	4.19 x 10^4	3.72 x 10^{-8}	5.0 x 10^3	1.86 x 10^{-4}
Mesolite[3]	7.65 x 10^{-5}	6.78 x 10^4	6.82 x 10^{-13}	1.0 x 10^{-2}	6.8 x 10^{-15}

[1] From a compilation by Sonnenthal and Spycher and (2001). All tabulated data are assumed applicable to both dissolution and precipitation kinetics.

[2] Rate constant at 167 ºC, the temperature of the initial experiment.

[3] The pre-exponential factor and activation energy for mesolite were assumed to be equal to that for albite.

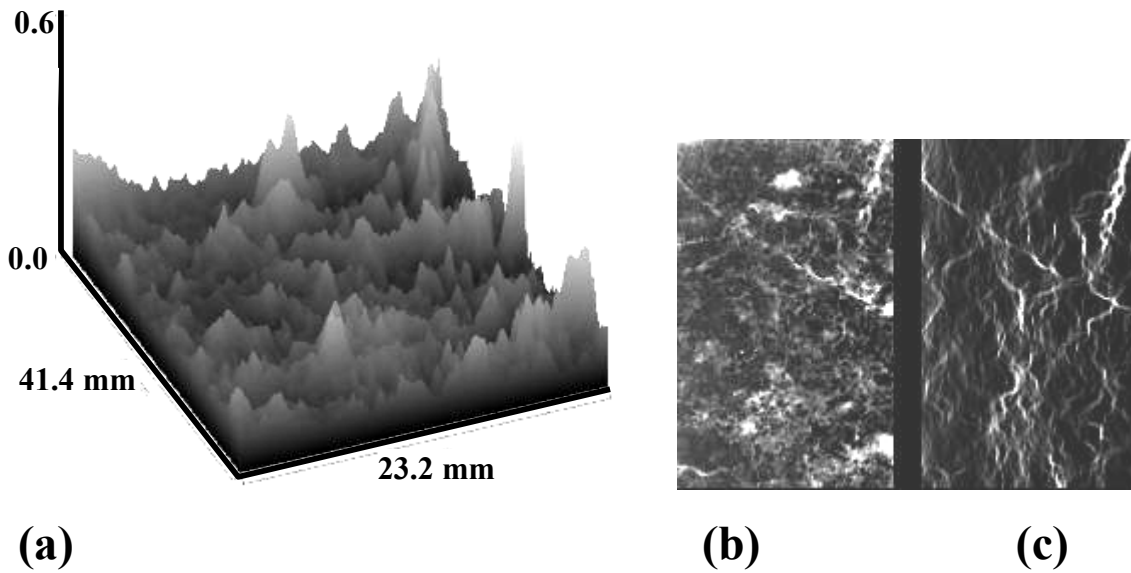**(a)**   **(b)**   **(c)**

Figure 1.   (a) Perspective view of fracture aperture calculated from high-resolution surface profilometry (30x vertical exaggeration). (b) Gray-scale image of fracture apertures (scale 0.0 mm (black); 0.25 mm (white)). (c) Simulations of fluid flow through the fracture yield estimates of local fluxes where the gray-scale (black through white) represents increasing fluxes. Flow direction is from top to bottom.
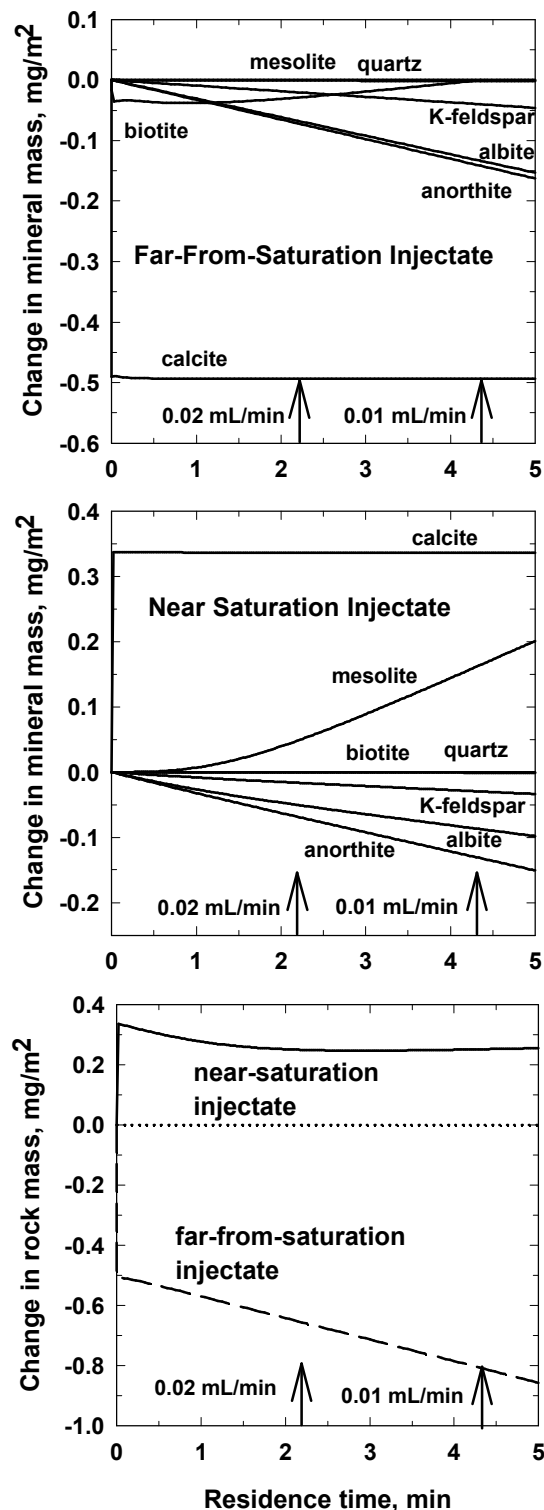
Figure 2.   Comparison of mineral and rock mass changes per square meter of fracture surface vs. fluid residence time (40-μm aperture) due to mineral dissolution and precipitation in a fracture for far-from-saturation (a) and near-saturation (b) fluid injectates. Net mass of rock precipitated or removed is shown in (c). Negative values indicate dissolution; positive values indicate precipitation.